

PACS numbers: 07.57.Hm; 78.20.Jq; 42.25.Hz
DOI: 10.1070/QE2015v045n05ABEH015774

Measurement of spatio-temporal field distribution of THz pulses in electro-optic crystal by interferometry method

P.A. Chizhov, A.A. Ushakov, V.V. Bukin, S.V. Garnov

Abstract. **We propose a scheme for measuring the spatial distribution of the THz pulse electric field strength in an electro-optic crystal using optical interferometry. The resulting images of the field distribution from a test source with a spherical wave front are presented.**

Keywords: *terahertz radiation, interferometry, electro-optical detection.*

1. Introduction

The development of THz radiation sources has made it possible to create new instruments for spectroscopy, tomography, imaging and microscopy [1–13]. Pulsed sources of THz radiation allow measurements in time-domain spectroscopy, e.g., using the electro-optical detection scheme [4, 6, 7]. The electro-optic crystal as a THz radiation detector is successfully applied for imaging [9]. In Refs [8, 12] chirped pulses were used that allow a single-pulse measurement of the entire THz field temporal profile, making it possible to reduce the image acquisition time. However, the imaging speed is mainly determined by the object spatial scanning time [9, 14] so that the main drawback of the electro-optical detection scheme is the use of small-aperture crystals. In the present paper we implement the imaging scheme based on an electro-optic crystal and using interferometric recording, which eliminates the necessity of scanning.

2. Imaging system in Thz range. Experimental setup

To generate and record the THz radiation we used a Spectra Physics Spitfire Pro XP laser system (centre wavelength, 800 nm; pulse repetition rate, 10 Hz; pulse duration, 40 fs; pulse energy, 2.5 mJ; Gaussian beam diameter at the $1/e^2$ level, 12 mm; horizontal polarisation). The laser radiation was divided into two parts. The main part was used to generate THz radiation in the source based on the optical breakdown in air induced by two-colour femtosecond laser pulses [15]. The other part of laser radiation – the probing pulse – after passing through the variable optical delay line was used to measure the electric field strength, as shown in Fig. 1.

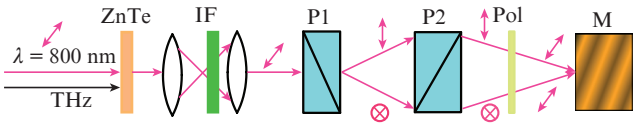

Figure 1. Schematic diagram of the experiment: (IF) interference filter; (P1) and (P2) Wollaston prisms; (Pol) film polariser; (M) CCD camera matrix.

The principle of THz radiation detection is based on the linear electro-optic effect. The THz pulse and the probing optical pulse (λ = 800 nm) were incident on the ZnTe crystal ($10 \times 10 \times 0.5$ mm, cut $\langle 110 \rangle$; vertical direction in the scheme corresponded to the $\langle 001 \rangle$ direction in the crystal). In this case, the polarisation of THz radiation was vertical, while the probing pulse was polarised at the angle 45°. As a result of the electro-optic effect in the optically isotropic ZnTe crystal the birefringence was induced, and in the above geometry of the experiment the probing radiation in the crystal was split into two waves (with vertical and horizontal polarisations and equal intensities), for which the difference between the refractive indices was linearly dependent on the electric field strength of the THz pulse.

The nonuniform distribution of the field strength over the crystal cross section caused the nonuniform distribution of the phase difference between the two waves at the output from the crystal. The purpose of the next-step registration scheme was to produce an interference pattern at the CCD matrix that carries the information about the phase difference distribution. To this end, the plane of the electro-optic crystal was imaged by a telescope consisting of two similar lenses (f = 20 cm) onto the matrix of the CCD camera (Basler acA2040-25gm-NIR, 1″, 2048 × 2048). Inside the telescope the interference filter was placed (the transmission centre wavelength, 795 nm; the bandwidth at the half-maximum level, 3 nm) aimed at increasing the coherence time of the probing femtosecond pulse, which made it possible to observe an interference pattern with a wide contrast area. The inter-

P.A. Chizhov A.M. Prokhorov General Physics Institute, Russian Academy of Sciences, ul. Vavilova 38, 119991 Moscow, Russia; e-mail: pvch@inbox.ru;
A.A. Ushakov A.M. Prokhorov General Physics Institute, Russian Academy of Sciences, ul. Vavilova 38, 119991 Moscow, Russia; Department of Physics, M.V. Lomonosov Moscow State University, Vorob'evy Gory, 119991 Moscow, Russia; e-mail: ushakov.aleksandr@physics.msu.ru;
V.V. Bukin, S.V. Garnov A.M. Prokhorov General Physics Institute, Russian Academy of Sciences, ul. Vavilova 38, 119991 Moscow, Russia; National Research Nuclear University 'MEPhI', Kashirskoe sh. 31, 115409 Moscow, Russia; e-mail: vladimir.bukin@gmail.com, svgarnov@mail.ru

Received 29 January 2015; revision received 13 February 2015
Kvantovaya Elektronika **45** (5) 434–436 (2015)
Translated by V.L. Derbov

ference pattern itself was produced by the interferometer consisting of two Wollaston prisms (with the beam separation angles 1.5° and 3°) and a polariser, oriented at the angle 45°. The use of two prisms with the beam separation angles of different magnitude and opposite sign allowed the formation of two orthogonally polarised waves in the CCD matrix plane, propagating at an angle to each other and, at the same time, imaging the electrooptic crystal plane without relative displacement. The polariser after Wollaston prisms ensures a similar polarisation of the waves, thereby providing their interference. In this way an interference pattern was formed at the CCD matrix with the period of fringes 30 μm, which corresponds to the convergence angle of interfering waves $\alpha = 1.5°$. The additional phase difference, caused by the electro-optic effect in the ZnTe crystal, lead to the shift of the fringes, i.e., to phase modulation of the observed pattern.

3. Data processing

In the course of experiments we obtained interferograms in the presence of a THz pulse (signal) and in its absence (reference). To increase the signal-to-noise ratio for each delay time between the optical pulse and the THz one, 50 signal and background records (frames) were made. The phase was reconstructed by processing the interferograms by means of the method based on filtration in the Fourier space [16]. As a result of the processing we obtained a two-dimensional map of the mean phase shift change caused by the presence of the THz pulse field. From the phase shift the THz electric field strength E_{THz} can be extracted. In correspondence with Ref. [17], if the polarisations of the THz pulse and optical radiation are oriented along the crystallographic axes of ZnTe, as in our experiment, then

$$E_{\mathrm{THz}} = \frac{\Gamma\lambda}{\pi d n^3 r_{41}} \simeq 55\Gamma \ [\mathrm{kV\ cm^{-1}}], \tag{1}$$

where Γ is the phase shift due to the THz field; λ is the probing radiation wavelength; n and r_{41} are the refractive index and the electro-optic coefficient of the crystal; and d is the crystal thickness.

4. Results

The spatio-temporal profiles of the THz pulse electric field, obtained in the experiments, are presented in Fig. 2. The electrooptic crystal was placed in the plane, separated by the distance of 1 cm from the geometric focal point of the Teflon

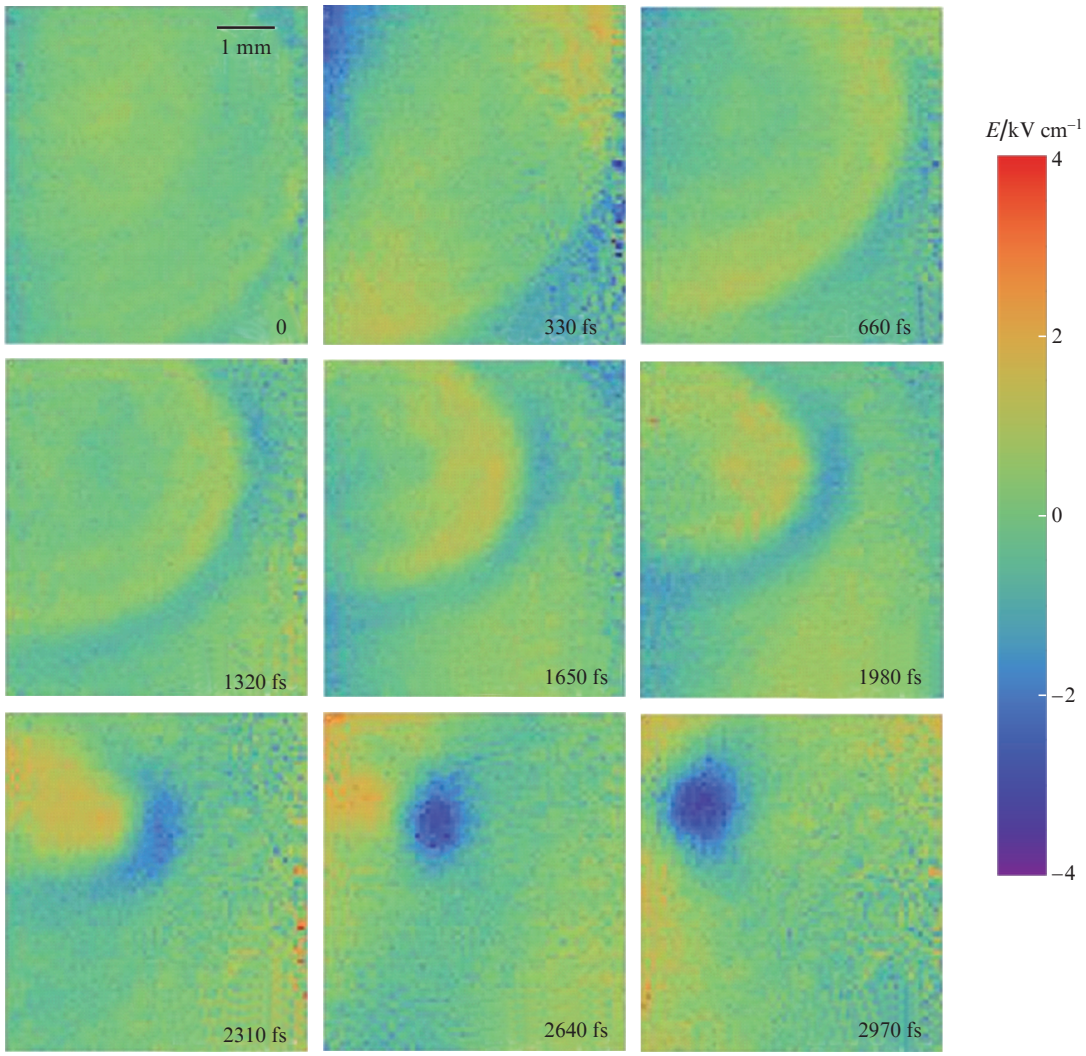

Figure 2. Images of the spatial distribution of the THz pulse electric field strength at different time delays.

lens. Because in this region the focused THz radiation has a spherical wave front, the profiles of the field strength E_{THz} have the shape of rings that correspond to the sections of the spherical wave front of the THz radiation by the planar wave fronts of the probing pulse. With growing delay time (i.e., for later arrival of the probing optical pulse) the ring diameter decreases, collapsing into a spot when the planar front of the probing pulse is tangent to the converging spherical front of the THz pulse.

The root-mean-square value of the noise component of the phase difference $\delta\varphi$ was calculated over the frame area, in which the signal was absent. The value obtained in this procedure, $\delta\varphi \simeq 5$ mrad, is equivalent to the value of the noise electric field strength $\delta E \simeq 280$ V cm^{-1}. In Refs [8, 9, 17] the minimal field detectable by the schemes based on shadow registration amounted to $\sim$100 V cm^{-1}. The main cause of the sensitivity loss in the interferometer scheme is the presence of mechanical vibrations that induce random shift of the fringes in the interference pattern. Minimisation of the mechanical vibration level is expected to increase the sensitivity level of the present technique.

5. Conclusions

We have proposed and implemented a scheme for measuring the spatio-temporal distribution of THz pulse electric field strength. The obtained field distributions from the test sources demonstrate the possibility of using this scheme in the problems of visualisation and imaging in the THz range, particularly, with relatively low-power radiation sources.

Acknowledgements. This work was supported by the Presidium of the Russian Academy of Sciences (Extreme Light Fields and Their Applications Programme), and the Stipend of the President of the Russian Federation for Young Scientists and Post-graduates (Project No. SP-2391.2013.2).

References

1. Zhang X.-C., Xu J. *Introduction to THz Wave Photonics* (New York: Springer, 2010).
2. Mittleman D.M., Hunsche S., Boivin L., Nuss M.C. *Opt. Lett*., **22** (12), 904 (1997).
3. Wynne K., Jaroszynski D.A. *Opt. Lett*., **24** (1), 25 (1999).
4. Wang S., Ferguson B., Abbott D., Zhang X.-C. *J. Biol. Phys*., **29** (2–3), 247 (2003).
5. Mittleman D.M., Gupta M., Neelamani R., Baraniuk R.G., Rudd J.V., Koch M. *Appl. Phys. B*, **68** (6), 1085 (1999).
6. Mittleman D.M., Jacobsen R.H., Nuss M.C. *IEEE J. Sel. Top. Quantum Electron*., **2** (3), 679 (1996).
7. Peiponen K.-E., Zeitler J.A., Kuwata-Gonokami M. *Terahertz Spectroscopy and Imaging* (Berlin: Springer-Verlag Berlin Heidelberg, 2013).
8. Jiang Z., Zhang X., Member S. *IEEE J. Quantum Electron*., **36** (10), 1214 (2000).
9. Jiang Z., Zhang X. *IEEE Trans. Microw. Theory Tech*., **47** (12), 2644 (1999).
10. Oh S.J., Choi J., Maeng I., Park J.Y., Lee K., Huh Y.-M., Suh J.-S., Haam S., Son J.-H. *Opt. Express*, **19** (5), 4009 (2011).
11. Hu B.B., Nuss M.C. *Opt. Lett*., **20** (16), 1716 (1995).
12. Jiang Z., Zhang X.-C. *Opt. Lett*., **23** (14), 1114 (1998).
13. Kim K.Y., Yellampalle B., Taylor A.J., Rodriguez G., Glownia J.H. *Opt. Lett*., **32** (14), 1968 (2007).
14. Kim K.Y., Yellampalle B., Rodriguez G., Averitt R.D., Taylor A.J., Glownia J.H. *Appl. Phys. Lett*., **88**, 041123 (2006).
15. Cook D.J., Hochstrasser R.M. *Opt. Lett*., **25** (16), 1210 (2000).
16. Takeda M., Ina H., Kobayashi S. *J. Opt. Soc. Am*., **72** (1), 156 (1982).
17. Casalbuoni S., Schlarb H., Schmidt B., Schmüser P., Steffen B., Winter A. *Phys. Rev. Spec. Topics-Accelerators and Beams*, **11** (7), 072802 (2008).